

Modeling of nonlocal electron kinetics in a low-pressure afterglow plasma

Robert R. Arslanbekov*

Department of Physics, Monash University, Clayton, Victoria 3168, Australia

Anatoly A. Kudryavtsev

Institute of Physics, St. Petersburg State University, St. Petersburg 198904, Russia

(Received 17 July 1998)

The electron kinetics in a low-pressure afterglow plasma is studied by means of the time- and space-dependent Boltzmann (kinetic) equation. A method based on the nonlocal approach is presented, which enables the nonlocal nature of the electron distribution function (EDF) to be accounted for in a simple manner, without solving a complicated kinetic equation. Simplified kinetic equations are derived, as well as some analytic solutions, for obtaining the EDF in terms of its energy-averaged parameters, such as the electron density and temperature. This allows an energy-balance equation to be used to describe the electron-energy decay at the kinetic level. To validate the proposed method, the full time- and space-dependent kinetic equation is solved numerically for an afterglow in Ar. It is observed that under nonlocal conditions the EDF is strongly non-Maxwellian. As a consequence, the values of the wall potential predicted using the kinetic approach differ drastically from those obtained on the premise of a Maxwellian EDF. Another striking nonlocal effect manifests itself in a strong spatial inhomogeneity of the electron temperature. The derived energy-balance equation coupled with the simplified nonlocal kinetic equations reproduce accurately both the spatial profiles and absolute values of the electron temperature obtained from the full kinetic simulations. An interesting phenomenon, obtained numerically and explained in terms of the nonlocal EDF, is that the radial fluxes of different portions of the EDF have opposite directions. A direct comparison between the fluid and kinetic approaches is carried out, and it is concluded that the fluid approach fails to describe correctly the essential properties of a low-pressure afterglow plasma, such as the temporal and spatial evolution of the electron temperature. It is further demonstrated that the volume-averaged (zero-dimensional) kinetic models can also lead to erroneous results in describing such plasmas. It is shown that superthermal electrons produced in processes involving metastables can have a great influence on the plasma decay, particularly on the wall potential and the diffusion-cooling rate. The present method has the advantage of being simple and semianalytic, and thus can be very useful in solving complex self-consistent problems. [S1063-651X(98)02312-5]

PACS number(s): 52.80.-s, 52.65.-y, 52.25.Dg

I. INTRODUCTION

There has been continuous interest in the afterglow (post-discharge) plasma during the past several decades. Both monatomic and molecular electropositive, as well as electronegative, afterglow plasmas have been intensively investigated. Recently, low-pressure afterglow plasmas have received increased attention owing to the development of power-modulated plasma sources (e.g., Refs. [1,2]) which offer a number of advantages for plasma processing. The formation of an ion-ion ("electronless") plasma has been observed in a low-pressure electronegative post-discharge plasma (e.g., Ref. [3]), which is also interesting from a practical point of view.

Owing to the fundamental and practical importance of the afterglow plasma, a great number of simulation models has been developed. The fluid models (also referred to as the continuum models) have been widely used to simulate the afterglow (e.g., Refs. [4-6]) and power-modulated (e.g., Ref. [2]) plasmas. The so-called global (volume-averaged) models of high-density, low-pressure discharges both for continuous wave and for pulsed-time excitation have recently

been proposed by Lieberman and co-workers (e.g., Refs. [1,7]). In both the fluid and global models, an *ad hoc* assumption of a Maxwellian electron distribution function (EDF) is made. There also exists a number of models in which a volume-averaged kinetic treatment is employed in order to predict zero-dimensional EDFs (e.g., Refs. [8,9]).

We present a kinetic study of a low-pressure afterglow plasma. In such a plasma the electron kinetics is essentially "nonlocal" and so knowledge of the spatial (and temporal) evolution of the EDF is of vital importance. In fact, estimations show that, for typical discharge conditions in Ar, the EDF at energies of interest is already "nonlocal" when the gas pressure is less than a few Torr (for a 1-cm-radius discharge). Since this study requires the solution of a complicated time- and space-dependent kinetic equation, it is highly desirable to develop a method that allows one to account for the nonlocal nature of the EDF in a simple and transparent manner. With this in mind, we take advantage of the powerful nonlocal approach proposed by Bernstein and Holstein [10] and Tsendin [11], which has recently received renewed attention (e.g., Refs. [12-17]) due to its physical clarity and simplicity and numerical efficiency. We also use techniques which we have developed for a negative-glow plasma which is similar in nature to the afterglow plasma (e.g., Ref. [18]).

The formulation of the problem is presented in Sec. II,

*Electronic address: Robert.Arslanbekov@sci.monash.edu.au

and the electron Boltzmann equation is introduced. We use the nonlocal approach to obtain simplified kinetic equations, and some analytic solutions, for describing the nonlocal EDF in terms of its energy-averaged parameters, namely, the electron density and temperature (mean energy) (Sec. II B). This represents a great advantage since these energy-averaged parameters can be found from the particle- and energy-balance equations, and thereby the need to solve the full kinetic equation is avoided (Secs. II C and II D). In Sec. III, we present a comparison between the fluid and kinetic approaches. The numerical results and discussion are presented in Sec. IV. Section V gives the summary and conclusions.

II. PROBLEM FORMULATION

We consider a low-pressure afterglow plasma. As in recent papers on nonlocal electron kinetics (e.g., Refs. [14,13,17]), a plasma is termed “low pressure,” when the electron energy-relaxation length λ_ϵ exceeds the discharge chamber characteristic dimension Λ (e.g., $\Lambda \approx R/2.4$ for a cylindrical geometry, where R is the tube radius), i.e., $\lambda_\epsilon > \Lambda$. We assume that the gas pressure p is not too low, so that the electron mean free path for momentum transfer λ_a is small compared to Λ , i.e., $\lambda_a < \Lambda$ (collisional regime). In principle, the analysis can be applied to describe the decay of any weakly ionized plasma after the input power has been turned off; such as the positive-column, microwave, RF, negative-glow, or other plasmas. Although we consider a collisional plasma, the present methodology and results can be extended to the (nearly) collisionless high-density plasmas (e.g., Refs. [1,7,2]). We assume a one-dimensional (1D) cylindrical geometry. The discharge wall is taken to be dielectric, so that the net flux of charges (electrons and ions) at the wall is zero. We restrict ourselves to the case of a rare-gas (electropositive) discharge. The plasma is considered to consist of two regions, namely, (i) the extensive quasineutral region, in which the space-charge (ambipolar) potential $\Phi(r)$ dominates and $n = n_i = n_e$ [where n is the plasma density and n_e (n_i) is the electron (ion) density] and (ii) the confined space-charge boundary sheath, which is not resolved spatially, and the presence of which is taken into account by using the appropriate boundary conditions. In the boundary sheath, a steep change (jump) $\Delta\Phi_w$ in the potential takes place which is necessary to confine most of the electrons and to balance total electron and ion currents to the (dielectric) wall.

A. Electron Boltzmann equation

In this section, we present the electron Boltzmann equation. The details of the kinetic formulation can be found in works by Tsendin (e.g., Refs. [11,19]) and in recently published papers (e.g., Refs. [12–17]). In what follows, we give a brief description only.

Since we consider a collisional plasma ($\lambda_a < \Lambda$), the conventional two-term expansion for the EDF can be employed: $f(\mathbf{v}, \mathbf{r}, t) = f_0(v, \mathbf{r}, t) + (\mathbf{v}/v) \cdot \mathbf{f}_1(v, \mathbf{r}, t)$, where f_0 is the isotropic part of the EDF, \mathbf{f}_1 its directed part ($|\mathbf{f}_1| \ll f_0$), \mathbf{v} the electron velocity ($v = |\mathbf{v}|$), and \mathbf{r} the spatial coordinate ($r = |\mathbf{r}|$). It is then convenient to use the total energy $\epsilon = w + e\Phi(\mathbf{r})$ (the sum of kinetic energy $w = \frac{1}{2}mv^2$ and potential

energy $e\Phi$) as an independent variable.

In the two-term expansion, the isotropic part of the EDF f_0 describes energy transfer in all kinds of collisional processes, whereas its directed part \mathbf{f}_1 describes momentum transfer in collisions with atoms. It is then possible to consider that \mathbf{f}_1 is quasistationary since its relaxation time is very short, i.e., of the order of ν_a^{-1} (where ν_a is the electron-atom collision frequency for momentum transfer). All plasma characteristics are assumed to be time dependent, such as the EDF itself, as well as the electron density and the electron temperature, as well as the space-charge potential profile, etc., i.e., $f_0 = f_0(\epsilon, \mathbf{r}, t)$, $n_e = n_e(\mathbf{r}, t)$, $T_e = T_e(\mathbf{r}, t)$, $\Phi = \Phi(\mathbf{r}, t)$, etc. For convenience, in most formulas that follow the index t is dropped. By representing the electron-electron ($e-e$) collision term and the electron-atom ($e-a$) elastic-recoil term in the Fokker-Planck form, one can write the time- and space-dependent kinetic equation for $f_0(\epsilon, \mathbf{r}, t)$ as

$$\frac{\partial f_0}{\partial t} = -\frac{1}{\sqrt{w}} \nabla \cdot \sqrt{w} \mathbf{J}_r + \frac{1}{\sqrt{w}} \frac{\partial}{\partial \epsilon} \sqrt{w} J_\epsilon + q^*, \quad (1)$$

where

$$\mathbf{J}_r(\epsilon, r) = \frac{1}{3} v \mathbf{f}_1 = -D_r \nabla f_0(\epsilon, r) \quad (2)$$

is the differential (i.e., energy- and space-resolved) flux in configuration space and $D_r = \frac{1}{3} \lambda_a v$ the electron diffusion coefficient,

$$J_\epsilon(\epsilon, r) = V_\epsilon f_0 + D_\epsilon \frac{\partial f_0}{\partial \epsilon} \quad (3)$$

is the differential flux in energy space, $V_\epsilon = V_e + V_a$ and $D_\epsilon = D_e + D_a$ are, respectively, the total dynamic-friction and diffusion coefficients, V_a (V_e) and D_a (D_e) represent, respectively, the dynamic-friction and diffusion coefficients in energy space due to $e-a$ ($e-e$) collisions, $V_e = 2\nu_e w A_1$ and $D_e = 2\nu_e w A_2$ with

$$A_1 = \frac{1}{n_e} \int_0^w f_0 \sqrt{w'} dw', \quad (4a)$$

$$A_2 = \frac{2}{3n_e} \left(\int_0^w f_0 w'^{3/2} dw' + w^{3/2} \int_w^\infty f_0 dw' \right), \quad (4b)$$

where ν_e is the frequency of $e-e$ Coulomb collisions, $V_a = \delta \nu_a w$ and $D_a = T_a V_a$, $\delta = 2m/M$ the fraction of electron energy lost in a single (quasi)elastic $e-a$ collision, and T_a the atom temperature. Other types of quasielastic collisions, such as collisions with ions (e.g., Ref. [20]) and molecules (e.g., excitation of vibrational or rotational states) (e.g., Ref. [21]), can also be included in the kinetic equation in the similar fashion.

The last term $q^*(w, r)$ in Eq. (1) describes the production of energetic (referred to as superthermal) electrons with $w \gg T_e$ in processes involving metastables, such as metastable-metastable (Penning) ionization and electron-metastable superelastic collisions. Under the plasma conditions of interest,

the q^* energy spectrum is very narrow and can adequately be approximated by a δ function (see Ref. [22] for details), which gives

$$q^*(w, r) = Q^*(r) \delta(w - w^*) / \sqrt{w}, \quad (5)$$

where $Q^*(r)$ is the integral rate at which superthermal electrons are generated and w^* is their energy; e.g., for the Penning-ionization process, $Q^*(r) = \beta_p n_m^2$ and $w^* = 2\epsilon_m - \epsilon_i$, where n_m is the metastable density, ϵ_m the metastable-state energy, ϵ_i the ionization potential, and β_p the corresponding rate constant [22].

The boundary conditions for Eq. (1) in a cylindrical geometry can be written as

$$\left. \frac{\partial f_0(\epsilon, r)}{\partial r} \right|_{r=r_{\text{acc}}(\epsilon), \epsilon \leq e\Phi_w} = 0. \quad (6)$$

Here, the first condition takes account of the radial symmetry, and the second condition describes reflection of electrons with $\epsilon \leq e\Phi_w$ at the $r = r_{\text{acc}}(\epsilon)$ boundary determined by $w(\epsilon, r) = 0$; Φ_w is the (full) wall potential, $\Phi_w = \Phi_{\text{sh}} + \Delta\Phi_w$, with $\Phi_{\text{sh}} = \Phi(R)$ being the space-charge potential at the boundary sheath. As such, $r_{\text{acc}}(\epsilon) = R$ for $\epsilon \geq e\Phi_{\text{sh}}$. For those electrons which can overcome the space-charge potential barrier ($\epsilon > e\Phi_w$) the boundary condition at the wall can be written as

$$\left(v f_0(\epsilon, r) \frac{\Delta\Omega}{4\pi} \right) \Big|_{r=R} = \left(-D_r(\epsilon, r) \frac{\partial f_0}{\partial r} \right) \Big|_{r=R}, \quad (7)$$

where

$$\Delta\Omega(\epsilon) = 2\pi \frac{1 - e\Delta\Phi_w/w}{1 + (e\Delta\Phi_w/w)^{3/2}} \quad (8)$$

is the effective loss cone with $w = \epsilon - e\Phi_{\text{sh}}$ (see Refs. [23,16] for details).

It is straightforward to include inelastic processes involving ground-state atoms (such as direct excitation and ionization) into the kinetic equation Eq. (1) (e.g., Refs. [11,15]). However, an inelastic process can be important for (trapped) electrons with $\epsilon \leq e\Phi_w$ only provided that its threshold ϵ^* is lower than the wall potential energy $e\Phi_w$; (free) electrons with $\epsilon > e\Phi_w$ are affected by inelastic processes to a lesser degree since they escape rapidly to the wall. Hence, when $e\Phi_w < \epsilon^*$, we can ignore such processes, while retaining a good approximation. Inelastic processes involving metastables (such as stepwise excitation and ionization), which typically have low thresholds, can be neglected in the kinetic equation compared with $e-e$ and $e-a$ collision processes (when $n_m/n_e \lesssim 20$, see Ref. [22]).

The EDF in Eq. (1) is normalized according to

$$n_e(r) = \int_{e\Phi(r)}^{\infty} \sqrt{\epsilon - e\Phi(r)} f_0(\epsilon, r) d\epsilon. \quad (9)$$

It is conventional to define the electron temperature T_e as $\frac{2}{3}$ of the mean kinetic energy:

$$T_e(r) = \frac{2}{3n_e} \int_{e\Phi(r)}^{\infty} w^{3/2} f_0(\epsilon, r) d\epsilon. \quad (10)$$

Although T_e can be introduced only when the EDF is Maxwellian, we adopt the definition of Eq. (10) in the present paper. In fact, in a low-pressure afterglow plasma, the EDF is close to Maxwellian only at thermal energies (where the rate of $e-e$ Coulomb collisions is high) and can be strongly non-Maxwellian at higher energies (see below).

The total spatial electron flux can then be calculated as

$$\Gamma_e(r) = - \int_{e\Phi(r)}^{\infty} \sqrt{w} D_r(\epsilon, r) \nabla f_0(\epsilon, r) d\epsilon. \quad (11)$$

It is appropriate to mention the following concerning the coefficients A_1 and A_2 of Eq. (4). These coefficients significantly complicate the kinetic equation (1) by making this equation nonlinear integrodifferential. However, some approximations are possible, which can be useful for analytic developments. It can be seen from Eq. (4) that $A_1 \rightarrow 1$ and $A_2 \rightarrow T_e(r)$ when $w \rightarrow \infty$. More precisely, numerical results showed that these coefficients can be approximated as

$$A_1(w, r) = \begin{cases} Aw/T_e(r), & w/T_e(r) \leq B, \\ 1, & w/T_e(r) > B, \end{cases} \quad (12)$$

$$A_2(w, r) = T_e(r) A_1(w, r),$$

where the constants A and B are determined by the shape of the EDF; for a Maxwellian EDF with T_e , $A \approx 0.385$, and $B \approx 2.6$ (e.g., Ref. [24]).

At this point, the kinetic equation (and its boundary conditions) has been specified and can be solved numerically. However, the direct solution of the full (nonlinear integrodifferential) time- and space-dependent kinetic equation (1) is a computationally intensive task especially when a self-consistent problem is to be treated. Hence, it is highly desirable to simplify the problem of finding the EDF. At the low pressures of interest, the key simplification is to use the nonlocal approach [10,11]. The nonlocal approach can be applied provided that $\lambda_\epsilon > \Lambda$. The following estimate of λ_ϵ can be obtained from the kinetic equation (1):

$$\lambda_\epsilon \approx \begin{cases} \lambda_a / \sqrt{\delta}, & \text{for Maxwellian electrons,} \\ \lambda_a \sqrt{\nu_a / (2\nu_e + \delta\nu_a)}, & \text{otherwise.} \end{cases} \quad (13)$$

Here, we take into account that for Maxwellian electrons, the $e-e$ dynamic-friction term is (almost) balanced by the $e-e$ diffusion term, i.e., $V_e f_0 + D_e \partial f_0 / \partial \epsilon \approx 0$; this is an equivalent condition for the zero Coulomb frequency ($\nu_e = 0$).

B. Nonlocal electron distribution function

The so-called nonlocal conditions are realized when $\lambda_\epsilon > \Lambda$ [11]. Under these conditions, the electrons transit radially without experiencing significant changes in total energy ϵ . The electrons can then be separated into two distinct groups, namely, *trapped* (with $\epsilon \leq e\Phi_w$) and *free* (with $\epsilon > e\Phi_w$), as described in the two following paragraphs.

The trapped electrons with a total energy ϵ can move only within a restricted (accessible) volume in the plasma $V_{\text{acc}}(\epsilon)$,

which is determined by $\epsilon \leq e\Phi(r)$. The explicit dependence of the trapped EDF on the spatial coordinate r is weak and hence the EDF can be expanded as $f_0(\epsilon, r) = f_0^{(0)}(\epsilon) + f_0^{(1)}(\epsilon, r)$, where $f_0^{(1)} \ll f_0^{(0)}$. A kinetic equation in total energy ϵ can be obtained for trapped electrons by using this expansion and performing spatial averaging of the kinetic equation (1) [11,15]. The trapped electrons transport a negligible current (spatial flux), despite the fact that they comprise the majority of electrons. Therefore, it should be stressed that the electron current (spatial flux) *cannot* be expressed in terms of the trapped EDF parameters, namely, n_e and T_e (see discussion in Sec. III). Moreover, under nonlocal conditions, different portions of the electron spectrum move radially almost independently ($\epsilon \approx \text{const}$), and their radial (spatial) fluxes may even have opposite directions (see Sec. IV and also Ref. [17]).

The free (also referred to as untrapped or unconfined) electrons are able to climb the space-charge potential barrier ($\epsilon > e\Phi_w$) and leave the plasma, thereby carrying the electron current. The free electrons cannot be described using a space-averaged kinetic equation, but their kinetic equation can also be simplified significantly. The reason is that the free electrons can be treated, with high accuracy, using the linear coefficients of Eq. (12), i.e., in terms of n_e and T_e . Under nonlocal conditions, the free electrons escape quickly to the wall; consequently, their EDF is strongly depleted (the free-electron density is low, $n_f \ll n_e$) and is essentially non-Maxwellian. One can show that even in the situation when $v_e > \delta v_a$ at $w \approx e\Phi_w = \eta T_e$ (where η is the wall potential energy in units of T_e), the free EDF is nonlocal (and hence non-Maxwellian) up to relatively high pressures. Indeed, the condition that $\lambda_\epsilon \approx \lambda_a \sqrt{v_a / (2v_e)} > \Lambda$ is satisfied for Ar when $p R^2 n_e < 5.7 \times 10^{11} \eta T_e$ (hereinafter, p is expressed in Torr, R in cm, n_e in cm^{-3} , and T_e in eV). For typical conditions in which $n_e = 10^{11} \text{ cm}^{-3}$, $\eta = 3-4$, $R = 1 \text{ cm}$, and $T_e = 1 \text{ eV}$, the above condition for nonlocality of the free EDF is fulfilled for $p \leq 10 \text{ Torr}$.

Having introduced the trapped and free electrons, we can derive their simplified kinetic equations. Before doing so, it is necessary to refer to the temporal behavior of the corresponding EDFs. The situation is straightforward for the free EDF since the relaxation time of a free electron with $\epsilon > e\Phi_w$ is very short, i.e., of the order of the free-diffusion time, $\tau_{fd} = \Lambda^2 / D_r \sim 10^{-7} - 10^{-6} \text{ s}$, which is much faster than the slow time of variation of $n_e(t)$ and $T_e(t)$. Hence, one can assume that the free EDF is quasistationary for $t \geq \tau_{fd}$ (where $t = 0$ corresponds to the start of the afterglow), i.e., its time dependence is via the slow variation of $n_e(t)$ and $T_e(t)$ [and also $n_m(t)$, $\Phi(t)$, etc.]. Strictly speaking, the trapped EDF cannot be treated as being quasistationary. However, since the time of the formation (shaping) of the trapped EDF [$\sim (2v_e + \delta v_a)^{-1}$] is shorter than the slow time of variation of n_e and T_e , as a first approximation it is possible to assume that the shape of the trapped EDF is determined by the instantaneous values of $n_e(r)$ and $T_e(r)$. Since we are most interested in the shape of the trapped EDF and calculate its energy-averaged parameters (n_e and T_e) from the particle- and energy-balance equations (see Secs. II C and II D), the above assumption of ‘‘quasistationarity’’ of the trapped EDF is justified.

Accordingly, we write the (quasistationary) space-averaged kinetic equation for the trapped electrons (see Refs. [11,13] for details):

$$\frac{d}{d\epsilon} \overline{\sqrt{w}} \left(V_\epsilon^{(0)} f_0^{(0)}(\epsilon) + D_\epsilon^{(0)} \frac{df_0^{(0)}(\epsilon)}{d\epsilon} \right) = 0, \quad (14)$$

where $V_\epsilon^{(0)}(\epsilon) = \overline{\sqrt{w} V_\epsilon} / \overline{\sqrt{w}}$ and $D_\epsilon^{(0)}(\epsilon) = \overline{\sqrt{w} D_\epsilon} / \overline{\sqrt{w}}$; the barred quantities $\overline{X}(\epsilon)$ designate spatial averages performed over the accessible volume $V_{\text{acc}}(\epsilon)$. This equation can be solved subject to the boundary conditions at $\epsilon = e\Phi_w$, which can be found in terms of the free EDF. In order to find the free EDF $f_{0f}(\epsilon, r)$ for $\epsilon > e\Phi_w$, a quasistationary kinetic equation with the linear coefficients A_1 and A_2 ($n_f \ll n_e$) can well be employed:

$$\frac{1}{r} \frac{\partial}{\partial r} \overline{\sqrt{w} r D_r} \frac{\partial f_{0f}}{\partial r} + \frac{\partial}{\partial \epsilon} \overline{\sqrt{w}} \left(\mathcal{V}_\epsilon f_{0f} + \mathcal{D}_\epsilon \frac{\partial f_{0f}}{\partial \epsilon} \right) + \overline{\sqrt{w} q^*} = 0, \quad (15)$$

where $\mathcal{V}_\epsilon = w(2v_e + \delta v_a)$ and $\mathcal{D}_\epsilon = w(2v_e T_e + \delta v_a T_a)$. This equation, subject to the boundary conditions (6) and (7), can be easily solved at any instant $t = t_0 > 0$ during the afterglow, given $n_e(r, t_0)$, $T_e(r, t_0)$, $\Phi(r, t_0)$, $\Phi_w(t_0)$, and $q^*(w, r, t_0)$.

The coupled nonlocal kinetic equations for the trapped [Eq. (14)] and free [Eq. (15)] electrons enable one to solve the problem of finding the complete EDF. The solution of this problem can be simplified by assuming that the free EDF for $e\Phi_w \leq \epsilon \leq e\Phi_w + T_e$ also depends only on ϵ . This can be done since the wall loss cone at these energies is yet small enough (i.e., $\Delta\Omega \ll 4\pi$) for these electrons to be ‘‘almost trapped.’’ Introducing a wall loss term into the space-averaged kinetic equation (14) gives (see Refs. [13,16] for details)

$$-\frac{d}{d\epsilon} \overline{\sqrt{w}} \left(V_\epsilon^{(0)} f_0^{(0)} + D_\epsilon^{(0)} \frac{df_0^{(0)}}{d\epsilon} \right) = \frac{\overline{\sqrt{w} f_0^{(0)}}}{\tau_w}, \quad (16)$$

where $\tau_w = \tau_w(\epsilon)$ is the characteristic time of escape to the wall for electrons with $\epsilon \geq e\Phi_w$:

$$\tau_w(\epsilon) \approx \frac{\Lambda^2}{D_r} + \frac{R}{2\bar{v}} \left(\frac{\Delta\Omega}{4\pi} \right)^{-1}. \quad (17)$$

It is straightforward to solve numerically the ordinary differential equation (16) in order to find the EDF $f_0^{(0)}(\epsilon)$, and thus the differential energy flux $J_\epsilon(\epsilon, r)$ at $\epsilon = e\Phi_w$. We can, however, simplify the problem even further by using approximate analytic solutions for the trapped and free electrons. Such a solution of Eq. (14) is

$$f_0^{(0)}(\epsilon) = C_n \{ \exp[\Psi(\epsilon)] + C_0 \}, \quad (18)$$

where C_n is the normalization constant, C_0 is an arbitrary constant, and $\Psi(\epsilon) = -\int_0^\epsilon d\epsilon' / T(\epsilon')$ with

$$T(\epsilon) = \frac{D_\epsilon^{(0)}(\epsilon)}{V_\epsilon^{(0)}(\epsilon)} \approx \frac{\tilde{T}_e w^{3/2} A_1 2v_e + T_a w^{3/2} \delta v_a}{w^{3/2} A_1 2v_e + w^{3/2} \delta v_a} \quad (19)$$

being the characteristic temperature of an electron with an energy ϵ and \tilde{T}_e being the temperature (local slope) of the Maxwellian part of the EDF (henceforward, we will use the ‘tilde’ over a quantity X , i.e., \tilde{X} , to denote that this quantity is related to the Maxwellian part of the EDF). Since the trapped EDF of Eq. (18) is a function only of ϵ , \tilde{T}_e is spatially uniform, i.e., $\tilde{T}_e = \text{const}$. Given the nonlocal EDF $f_0^{(0)}(\epsilon)$, it is possible to establish the link between $T_e(r)$ and \tilde{T}_e when the EDF is close to Maxwellian $T_e(r) \approx \tilde{T}_e$.

It readily follows from Eq. (19) that, in the energy region where e - e Coulomb collisions are dominant ($2\nu_e \gg \delta\nu_a$), $T(\epsilon) \approx \tilde{T}_e$ and, hence, the trapped EDF of Eq. (18) in this region is Maxwell-Boltzmann

$$\tilde{f}_0(\epsilon) = \frac{2}{\sqrt{\pi}} \frac{n_{e0}}{\tilde{T}_e^{3/2}} \exp(-\epsilon/\tilde{T}_e), \quad (20)$$

where the constant C_0 [being important only at energies close to $e\Phi_w$, see Eq. (23) below] is neglected and n_{e0} is the electron density at the position of zero reference potential ($r=0$ for a cylindrical geometry).

In order to find the constant C_0 in Eq. (18), one can apply a zero boundary condition $f_0^{(0)} = 0$ at $\epsilon = e\Phi_w$, which yields $C_0 = -\exp[\Psi(e\Phi_w)]$. However, since in reality the EDF does not vanish for $\epsilon > e\Phi_w$, this approximation allows only very crude estimates of the EDF and the energy flux [$J_\epsilon(\epsilon, r)$, see Eq. (25) below] at $\epsilon \approx e\Phi_w$. In order to improve the accuracy of the calculations, one can use a nonzero boundary condition at $\epsilon = e\Phi_w$, in terms of the free EDF. Since the free EDF for $\epsilon > e\Phi_w$ falls off sharply with increasing energy, the dynamic-friction term $V_\epsilon^{(0)} f_0^{(0)}$ in Eq. (16) is smaller than the diffusion term $D_\epsilon^{(0)} df_0^{(0)}/d\epsilon$ and, as a first approximation, can be neglected. We can then write an estimate of the free EDF as

$$f_{0f}(\epsilon) \approx C_f \exp(-\epsilon/T_f). \quad (21)$$

Here, C_f is the normalization constant and $T_f = \frac{1}{2} \Delta\epsilon$ is the free-electron ‘temperature,’ where $\Delta\epsilon$ is the energy change experienced by an electron with $\epsilon = e\Phi_w$ during the time τ_w [see Eq. (17)] it escapes to the wall:

$$\Delta\epsilon \approx \sqrt{4D_\epsilon^{(0)} \tau_w}. \quad (22)$$

A total electron energy of $\epsilon \approx e\Phi_w + \Delta\epsilon$ must be substituted into the right-hand side of Eq. (22), thus yielding an algebraic equation for $\Delta\epsilon$. We can now find the desired constant C_0 in Eq. (18) by matching the EDFs, and the energy fluxes, for $\epsilon \leq e\Phi_w$ [Eq. (18)] and $\epsilon \geq e\Phi_w$ [Eq. (21)], which gives

$$f_0^{(0)} \approx C_n \left\{ \exp[\Psi(\epsilon)] - \left[\exp(\Psi) \left(1 - \frac{T_f}{T} \right) \right]_{e\Phi_w} \right\}. \quad (23)$$

Given the nonlocal EDF $f_0^{(0)}(\epsilon)$, the small perturbation term $f_0^{(1)}(\epsilon, r)$, and thus the differential spatial flux $J_r^{(1)}(\epsilon, r)$, can be found from a quasistationary kinetic equation for the trapped electrons (see Ref. [11] for details)

$$J_r^{(1)} = -D_r \nabla f_0^{(1)} = \frac{1}{r} \int_0^r \frac{\partial}{\partial \epsilon} (\sqrt{w} J_\epsilon^{(0)}) r' dr', \quad (24)$$

where $J_\epsilon^{(0)}(\epsilon, r)$ is the differential energy flux of Eq. (3) in terms of the nonlocal EDF $f_0^{(0)}(\epsilon)$:

$$J_\epsilon^{(0)}(\epsilon, r) = V_\epsilon(\epsilon, r) f_0^{(0)}(\epsilon) + D_\epsilon(\epsilon, r) \frac{df_0^{(0)}(\epsilon)}{d\epsilon}. \quad (25)$$

The total electron flux consists of two fluxes, namely,

$$\Gamma_e(r) = \Gamma_e^{(t)}(r) + \Gamma_e^{(f)}(r), \quad (26)$$

where $\Gamma_e^{(t)} = \Gamma_e(\epsilon \leq e\Phi_w)$ is the trapped-electron flux (integral of $J_r^{(1)}$) and $\Gamma_e^{(f)} = \Gamma_e(\epsilon \geq e\Phi_w)$ is the free-electron flux. The free-electron flux, in its turn, also consists of two fluxes

$$\Gamma_e^{(f)}(r) = \Gamma_e^{(\epsilon)}(r) + \Gamma_e^{(s)}(r), \quad (27)$$

where $\Gamma_e^{(s)} = (1/r) \int_0^r Q^*(r') r' dr'$ is the flux of superthermal electrons with $\epsilon > e\Phi_w$ and $\Gamma_e^{(\epsilon)}$ is the electron flux out of the potential well ($\epsilon \leq e\Phi_w$)

$$\Gamma_e^{(\epsilon)}(r) = \frac{1}{r} \int_0^r \sqrt{w} J_\epsilon^{(0)}(\epsilon, r') |_{\epsilon=e\Phi_w} r' dr', \quad (28)$$

where we approximated $J_\epsilon(\epsilon, r) \approx J_\epsilon^{(0)}(\epsilon, r)$.

In the nonlocal approach, the differential energy flux $J_\epsilon(\epsilon, r)$ at $\epsilon = e\Phi_w$ has the physical meaning: $J_\epsilon(\epsilon, r)$ (and so $\Gamma_e^{(\epsilon)}$) determines the rate of the electron flow out of the trapped ‘reservoir’ ($\epsilon \leq e\Phi_w$) into the ‘sink’ region ($\epsilon > e\Phi_w$) via the ‘orifice’ in energy space at $\epsilon = e\Phi_w$. Provided that the fluxes of trapped and superthermal electrons are small, all the electron current is due to $\Gamma_e^{(\epsilon)}$, i.e., $\Gamma_e \approx \Gamma_e^{(\epsilon)}$. To quantify the contribution of superthermal electrons to the total electron flux, it is convenient to introduce the ratio $\gamma = \Gamma_e^{(s)}/\Gamma_e$, e.g., $\gamma \rightarrow 1$ when almost all the electron flux is transported by superthermal electrons (see Sec. II E).

C. Description of the ions and the space-charge potential profile

In the present paper, the plasma is considered to contain only positive ions. The ions can be satisfactorily described in the fluid approximation by employing the continuity equation

$$\frac{\partial n_i}{\partial t} + \nabla \cdot \Gamma_i = Q_i^*, \quad (29)$$

where Q_i^* represents the ion production rate in processes involving metastables (e.g., Penning ionization) and the ion (particle) flux is

$$\Gamma_i = -D_i \nabla n_i - n_i \mu_i E. \quad (30)$$

Here, $E = -\nabla\Phi$ is the space-charge electric field, D_i the ion diffusion coefficient, and μ_i the ion mobility; $D_i/\mu_i = T_i/e$ with T_i being the ion temperature (here, $T_i = T_a$).

The link between the plasma-density and space-charge potential profiles, $n(r) = n[\Phi(r)]$, can be established by Eq.

(9) via the nonlocal EDF $f_0^{(0)}(\epsilon)$. Only when the relationship between these profiles has the Boltzmann form, i.e., $n \propto \exp(-e\Phi/T_e)$, does the expression (30) for the ion flux reduce to its familiar form

$$\Gamma_i = -D_i(1 + T_e/T_a)\nabla n_i = -D_{\text{amb}}\nabla n_i, \quad (31)$$

where D_{amb} is the ambipolar-diffusion coefficient. Provided that Eq. (31) is satisfied, Eq. (29) is a linear diffusion equation. In general, Eqs. (29) and (30) coupled with Eq. (9) result in a nonlinear equation for $n(r,t)$ [and $\Phi(r,t)$] (see Ref. [11] for details). Since we do not solve a self-consistent problem, we assume that Eq. (31) is satisfied.

The Bohm boundary condition can be used for Eq. (29): $\Gamma_{iw} = n_{iw}v_B$, where $v_B = \sqrt{T_{ew}/M}$ is the Bohm velocity [hereinafter, the subscript w in X_w will denote that $X(r)$ is evaluated at the wall, i.e., $X_w = X(r=R)$]. This condition yields the ratio χ of the plasma density at the discharge center (n_0) to that at the wall (n_w) as $\chi = n_0/n_w \approx (2\Lambda/\lambda_i)\sqrt{T_a/T_{ew}}$, where λ_i is the ion mean free path.

In order to calculate the space-charge potential profile $\Phi(r)$, a self-consistent problem must be solved. This can be done by coupling the Boltzmann equation for the electrons, the continuity equation for the ions, and Poisson's equation. To avoid having to solve the space-dependent Boltzmann equation, e.g., in the fluid approach, the electron flux (Γ_e) is represented in terms of n_e and T_e . However, since such a representation cannot be employed (see Sec. III), the problem cannot be simplified by this means. Moreover, the direct solution of Poisson's equation is complicated by the fact that it involves a small difference between two large values (n_e and n_i), which requires high-precision (and high-stability) numerical schemes (e.g., Ref. [2]). It is thus far more convenient to divide the discharge volume spatially into a quasineutral plasma and a space-charge boundary sheath. In the quasineutral plasma, Poisson's equation is redundant, the space-charge potential profile $\Phi(r)$ can be found from the continuity equation for the ions [Eqs. (29) and (30)], and the plasma-density profile $n(r)$ can then be calculated from Eq. (9) (see Refs. [11,13] for details). The boundary sheath (in which the potential jump $\Delta\Phi_w$ occurs) can be considered to be infinitely thin and fully collisionless for the electrons, and hence does not have to be resolved spatially.

For the purposes of studying the electron kinetics, knowledge of the exact, self-consistent space-charge potential profile $\Phi(r)$ is not necessary. Moreover, the nonlocal trapped EDF (being a function only of ϵ) should not be sensitive to the exact shape of $\Phi(r)$. This is also true for the free electrons with $\epsilon > e\Phi_w > e\Phi(r)$. Hence, a model $\Phi(r)$ can be used, for which an approximate expression can be obtained by assuming that the EDF is close to Maxwellian with T_e and that the plasma-density profile is Bessel-like, which gives

$$\Phi(r) = (T_e/e)\ln[\chi + (1-\chi)J_0(2.4r/R)], \quad (32)$$

where J_0 is the zeroth-order Bessel function. As such, $\Phi_{\text{sh}} = (T_e/e)\ln\chi$.

The wall potential jump $\Delta\Phi_w$, or the (full) wall potential $\Phi_w = \Phi_{\text{sh}} + \Delta\Phi_w$, can be calculated by equating the electron flux at the wall [Γ_{ew} of Eq. (11)] to the ion flux [Γ_{iw} of Eq.

(30)]. Using the complete definitions of these fluxes complicates finding $\Delta\Phi_w$. In order to avoid a complicated solution, we can use the approximate expression for the ion flux [Eq. (31)] and the nonlocal approach for finding the EDF (see Sec. II B) to obtain the following equation for Φ_w :

$$\Gamma_{iw} = \frac{1}{(1-\gamma_w)R} \int_0^R \sqrt{w} J_\epsilon^{(0)}(\epsilon, r')|_{\epsilon=e\Phi_w} r' dr'. \quad (33)$$

Here, the differential energy flux $J_\epsilon^{(0)}$ is given by Eq. (25) in which the nonlocal EDF $f_0^{(0)}(\epsilon)$ can be found by using the techniques derived in Sec. II B. The simplest technique consists in employing the analytic EDF $f_0^{(0)}(\epsilon)$ of Eq. (23) in Eq. (33), which thus gives a simple transcendental equation for Φ_w . In order to obtain an estimate of Φ_w , one can apply a zero boundary condition at $\epsilon = e\Phi_w$ for the EDF of Eq. (18) [i.e., $f_0^{(0)}(\epsilon = e\Phi_w) = 0$], which yields [25]

$$\Phi_w \approx \frac{\tilde{T}_e}{e} \ln \left[\left(\frac{e\Phi_w}{\tilde{T}_e} \right)^{3/2} (\tau_{\text{amb}}\nu_e)(1-\gamma_w)^{-1} \right]_{e\Phi_w}, \quad (34)$$

where the right-hand side is to be evaluated at $\epsilon \approx e\Phi_w$, $\nu_e = \langle \nu_e \rangle + \delta\nu_e T_a / (2\tilde{T}_e)$, and $\tau_{\text{amb}} = \Lambda^2 / D_{\text{amb}}$ is the ambipolar-diffusion time.

One can now see from Eq. (34) that Φ_w (and hence $\Delta\Phi_w$) is a function of the plasma parameters, i.e., $\Phi_w = \Phi_w(n_e, \tilde{T}_e, p, \gamma_w, R, \dots)$. Since typically $\nu_e \approx \langle \nu_e \rangle$, the value of Φ_w is determined essentially by the product $\tau_{\text{amb}}\langle \nu_e \rangle$ at $w \approx e\Phi_w$; provided that this product is not large, the values of the potential jump $\Delta\Phi_w = \Phi_w - \Phi_{\text{sh}}$ can be as low as $\sim T_e/e$ (for $\gamma_w = 0$), as has been predicted in Ref. [26]. Conversely, when $\gamma_w = \gamma(R) \rightarrow 1$ [see Eq. (34)], anomalously high potential jumps $\Delta\Phi_w$ can occur (see Refs. [25,22] and Sec. II E). These results contradict those obtained on the premise of a Maxwellian EDF, which yield no dependence of $\Delta\Phi_w$ on the major plasma parameters and predict that $\Delta\Phi_w \gg T_e/e$ [see Eq. (49) and discussion in Sec. III below].

D. Energy balance of the trapped electrons

In order to find the electron temperature (or the mean energy), an energy-balance equation can be derived. However, this equation can be obtained and used only when the EDF (or its shape) is known via its parametric dependence on T_e ; otherwise, when no such knowledge is available, an energy-balance equation cannot be used and a full kinetic equation must be solved. Since we have derived techniques for obtaining the trapped EDF in terms of T_e (and n_e) (see Sec. II B), we can indeed use an energy-balance equation.

Since under nonlocal conditions the electron ensemble consists of two distinct groups (namely, trapped-free) which exhibit different behaviors both in energy and in configuration spaces, an energy balance of all electrons *cannot* give T_e (see also discussion in Sec. III). Instead, an energy balance of the trapped electrons must be considered, for which the associated equation can be obtained by multiplying the kinetic equation (1) by $w(\epsilon, r)$ and integrating over the energy interval $\epsilon \leq e\Phi_w$. Under nonlocal conditions ($\lambda_\epsilon > \Lambda$), the whole plasma volume contributes to the electron temperature

formation, and it is useful to perform spatial averaging of a space-dependent energy-balance equation. Keeping only the main terms, one then gets

$$\frac{\partial}{\partial t} \left(\frac{3}{2} \langle n_e T_e \rangle \right) = \langle H_{dc} \rangle + \langle H_{ea} \rangle + \langle H_s \rangle, \quad (35)$$

where $\langle \dots \rangle$ denotes spatial (volume) averaging and H_s is the heating rate of the trapped electrons in Coulomb collisions with superthermal electrons (see Sec. II E). The two remaining terms in Eq. (35), together with the two terms which were neglected, are described below.

In Eq. (35), $H_{dc} = H_{dc}^{(0)}$ is the diffusion-cooling term:

$$H_{dc}^{(0)}(r) = w^{3/2} J_e^{(0)}(\epsilon, r) \Big|_{\epsilon = e\Phi_w}. \quad (36)$$

Conceptually, H_{dc} represents the rate of transport of energy to the wall by those electrons which can overcome the space-charge potential barrier. For the trapped electrons, diffusion cooling thus occurs due to the energy outflow in *energy* space at $\epsilon = e\Phi_w$, and not due to spatial diffusion against the space-charge field in the plasma and in the boundary sheath. The latter mechanism is a result of the spatial inhomogeneity of the trapped EDF ($\propto f_0^{(1)}$) and its rate is

$$H_{dc}^{(1)}(r) = \int_{e\Phi(r)}^{e\Phi_w} w \nabla \cdot (\sqrt{w} D_r \nabla f_0^{(1)}) d\epsilon. \quad (37)$$

It can be shown that this term is small compared with H_{dc} and hence can be neglected. Indeed, as an upper estimate, $\langle H_{dc}^{(1)} \rangle \approx \langle e\Gamma_e^{(1)} E \rangle$, whereas $\langle H_{dc}^{(0)} \rangle \approx \langle e\Gamma_e E \rangle$ [see Eq. (38) below], hence $\langle H_{dc}^{(1)} \rangle / \langle H_{dc}^{(0)} \rangle \approx \Gamma_e^{(1)} / \Gamma_e \ll 1$. It is interesting to note that the diffusion cooling as a result of spatial motion, i.e., $H_{dc}^{(1)}$, may become the ‘‘diffusion heating’’ when the trapped-electron flux is inwardly directed, i.e., $\Gamma_e^{(1)} < 0$. By contrast, the diffusion cooling resulting from motion in energy space is always cooling, i.e., $H_{dc}^{(0)} < 0$. Taking into account that $H_{dc}(r) = -w(e\Phi_w, r) \nabla \cdot \Gamma_e^{(\epsilon)}$, one can obtain the diffusion-cooling rate in a more explicit form:

$$\langle H_{dc} \rangle = -(2/R) e \Delta \Phi_w \Gamma_{ew}^{(\epsilon)} + \langle e\Gamma_e^{(\epsilon)} E \rangle, \quad (38)$$

where the first and second terms can be identified with, respectively, energy losses resulting from diffusion against the space-charge field in the boundary sheath and in the plasma ($E < 0$); in other words, H_{dc} represents the work that the (trapped) electrons do on this electric field. It can be seen from Eq. (38) that the diffusion-cooling rate is sensitive to the amount of electron flux carried by superthermal electrons since $H_{dc} \propto (1 - \gamma) \Gamma_e$; e.g., when $\gamma = 1$, $H_{dc} = 0$ (see discussion in Sec. II E). Only when the contribution of superthermal electrons to Γ_e is small (i.e., $\gamma = 0$) does H_{dc} reduce to its familiar form

$$\langle H_{dc} \rangle = -(2/R) \Delta \Phi_w j_w + \langle jE \rangle, \quad (39)$$

where $j = j_e = j_i$ with $j_e = e\Gamma_e$ ($j_i = e\Gamma_i$) being the electron (ion) current density.

In Eq. (35), H_{ea} represents the rate of exchange of energy as a result of elastic-recoil collisions between the trapped

electrons and atoms; this term can be calculated using the trapped EDF $f_0^{(0)}(\epsilon)$ of Eq. (23):

$$H_{ea}(r) = - \int_{e\Phi(r)}^{e\Phi_w} \sqrt{w} \left(V_a f_0^{(0)} + D_a \frac{df_0^{(0)}}{d\epsilon} \right) d\epsilon. \quad (40)$$

Only when the trapped EDF is close to Maxwellian [i.e., $f_0^{(0)} = \tilde{f}_0$ of Eq. (20)], does this expression for H_{ea} reduce to its familiar form [see Eq. (46) below]; otherwise Eqs. (40) and (46) may differ significantly. It is then possible to show that for heavy gases (such as Ar, Kr, etc.), in which the thermal contact between electrons and atoms is ‘‘poor’’ (due to the small values of δ and ν_a at low energies), the rate of cooling in *e-a* collisions becomes smaller than the diffusion-cooling rate (i.e., $H_{ea} \ll H_{dc}$), when T_e is not high and the pressure is low. This fact was invoked in the literature to describe the situation in which T_e falls below T_a in a low-pressure afterglow plasma (see Refs. [5,26] for details).

In writing Eq. (35) we also neglected cooling of the trapped electrons that arises from Coulomb collisions with free electrons, for which the rate is

$$H_f(r) = \int_{e\Phi_w}^{\infty} \sqrt{w} \left(V_e f_{0f} + D_e \frac{\partial f_{0f}}{\partial \epsilon} \right) d\epsilon. \quad (41)$$

It is easy to calculate this rate in terms of the free EDF $f_{0f}(\epsilon, r)$ from Eq. (15). However, due to fact that the density of free electrons, n_f , is low [they escape to the wall very quickly, $n_f \approx (\tau_{fd} / \tau_{amb}) n_e \ll n_e$], H_f is small. Indeed, one can show that $H_f \approx 2\nu_e(e\Phi_w) e\Phi_w n_f (1 - T_e / T_f)$, where $T_f < T_e$ and so $H_f < 0$. Since $\Gamma_{ew} \approx (R/2) n_f / \tau_{fd}$, one obtains $H_f / H_{dc} \approx -2\nu_e(e\Phi_w) \tau_{fd} (1 - T_e / T_f) \ll 1$ since $2\nu_e(e\Phi_w) \tau_{fd} \ll 1$ under nonlocal conditions. Hence, for the sake of simplicity, we have neglected this term. Note that in a steady-state negative-glow plasma in the presence of an ionization source, there exists a substantial hot-electron population with $T_f \gg T_e$ (for $w \leq \epsilon^*$), and trapped electrons can be heated efficiently ($H_f > 0$), instead of being cooled, in Coulomb collisions with these hot electrons (e.g., Ref. [18]).

Other mechanisms to be included into the energy-balance equation (35) are inelastic processes involving ground-state atoms (e.g., direct or stepwise excitation and ionization) (see also Sec. II E). However, only inelastic processes with (low) thresholds $\epsilon^* < e\Phi_w$ are to be considered; those with $\epsilon^* \geq e\Phi_w$ do not affect the energy balance of the trapped electrons with $\epsilon \leq e\Phi_w$.

E. Influence of the superthermal electrons

The processes involving metastables result in the production of energetic (superthermal) electrons with $w \gg T_e$. The importance of superthermal electrons in electron-energy decay has been pointed out already in early studies (e.g., Refs. [27,24]). More recently, it has been concluded that these electrons can have a vital influence on the wall potential and the diffusion-cooling rate [25,22]. The heating rate [H_s in Eq. (35)] of the trapped electrons by superthermal electrons can be calculated as (see Refs. [24,25,22,18] for more details)

$$H_s(r) \approx \int_{e\Phi_w}^{\infty} \sqrt{w} V_e f_{0s} d\epsilon = Q^*(r) \epsilon_{\text{eff}}^*(r), \quad (42)$$

where $f_{0s} = f_{0s}(\epsilon, r)$ is the superthermal EDF [$\propto q^*$ in Eq. (1)] and ϵ_{eff} is the effective energy (in units of eV) transferred to the trapped electrons in Coulomb collisions with superthermal electrons; it can be estimated as (when $w^* > e\Phi_w$)

$$\epsilon_{\text{eff}}^* \approx w^* (2\nu_e \tau_{\text{fd}}) |_{w=w^*}. \quad (43)$$

Hence, only a fraction (determined by the product $2\nu_e \tau_{\text{fd}}$ at $w = w^*$) of the superthermal energy w^* goes into heating of the trapped electrons. For example, the higher n_e is (or ν_e), the larger this fraction is; whereas the quicker the superthermal electrons escape to the wall (the shorter τ_{fd}), the smaller this fraction is. Therefore, correct values for H_s can be obtained only at the kinetic level (see Ref. [18] and Sec. II F).

Let us now discuss briefly the influence of superthermal electrons on the wall potential (Φ_w) and the diffusion-cooling rate (H_{dc}) (see Refs. [25,22] for details). It can be seen from the expressions for Φ_w [Eq. (34)] and $\langle H_{\text{dc}} \rangle$ [Eq. (38)] that they both contain the factor $(1 - \gamma_w)$: $\Phi_w \propto -\ln(1 - \gamma_w)$ and $\langle H_{\text{dc}} \rangle \propto (1 - \gamma_w)$. Hence, account was taken of the fact that the flux $\Gamma_e^{(\epsilon)}$ out of the potential well is less than the total electron flux $\Gamma_e (= \Gamma_i)$ by an amount equal to the flux of (free) superthermal electrons $\Gamma_e^{(s)}$ [see Eq. (27)] (note that $\Gamma_e^{(t)} = 0$ at the wall). When γ_w is increased, the diffusion-cooling rate is reduced [despite the increase in the wall potential Φ_w , see Eq. (34)] and as $\gamma_w \rightarrow 1$, $\langle H_{\text{dc}} \rangle \rightarrow 0$. Physically this means that as $\gamma_w \rightarrow 1$, $e\Phi_w$ increases to a value ($\sim w^*$) at which most of the bulk electrons are trapped inside the discharge volume. In this case the (free) superthermal electrons ensure equality of the ion and electron fluxes at the wall, as well as energy expenditures in maintaining the space-charge field in the plasma and the potential jump in the boundary sheath. Since the superthermal electrons obtain energy from excited states, diffusion cooling of the trapped electrons “shuts off” under these conditions. During the transition from $\gamma_w \ll 1$ to $\gamma_w = 1$, the diffusion cooling is gradually reduced, since the part of the work required to maintain the space-charge field comes from potential energy stored in excited atoms.

Finally, it should be mentioned that, although it is possible to neglect the processes involving metastables in the kinetic equation (see Sec. II A), these processes, such as stepwise excitation (and de-excitation) and ionization, can be important in the energy balance of the trapped electrons (e.g., Refs. [22,9]). Typically for rare gases, the lowest metastable state is the most populated, and stepwise excitation from this state to the nearest metastable or resonance states may represent an efficient cooling mechanism. Note also that heating produced by recombination, in which an energy release of the order of T_e per electron occurs, can be ruled out owing to the low gas pressures.

F. Comparison with the volume-averaged kinetic models

The importance of the nonlocal nature of the electron spectrum in describing low-pressure plasmas is now well understood (e.g., Refs. [11–14,17,19,18]). There exists, how-

ever, a number of models which employ a volume-averaged kinetic treatment to obtain spatially uniform (zero-dimensional) EDFs (e.g., Refs. [8,9]). In order to account for the removal of electrons to the wall, the spatial-diffusion term in a volume-averaged (zero-dimensional) kinetic equation is often written in the τ approximation (e.g., Refs. [8,9]): $\nabla \cdot (D_r \nabla f_0) \approx -f_0 / \tau_{\text{char}}$. Some models (e.g., Ref. [9]) take the ambipolar-diffusion time τ_{amb} , as the characteristic removal time τ_{char} , i.e., $\tau_{\text{char}}(w) \approx \tau_{\text{amb}}$ (see also Ref. [5]). Thus, such models assume that *all* electrons diffuse to the wall at the *same* rate $\propto \tau_{\text{amb}}$. In reality, however, free electrons diffuse to the wall in a free-diffusion time (τ_{fd}) which is shorter than τ_{amb} by orders of magnitude (i.e., $\tau_{\text{fd}} \ll \tau_{\text{amb}}$); by contrast, the lifetime of a trapped electron can be substantially lower than τ_{amb} . Only on average does the diffusion time of an electron ensemble match τ_{amb} . Attempts to introduce more complicated (energy-dependent) expressions for $\tau_{\text{char}}(w)$ (e.g., Ref. [8]) do not improve the accuracy of such models. The volume-averaged kinetic treatment under nonlocal conditions may lead to erroneous results, as illustrated in the two following examples.

The first example is that a volume-averaged kinetic model does not allow one to obtain correct values for the heating rate H_s in Eq. (35). Indeed, such a model predicts that the removal of superthermal electrons takes place in a slow time of τ_{amb} , and so that $\epsilon_{\text{eff}}^* \approx w^* (2\nu_e \tau_{\text{amb}})$ [see Eq. (43)]. Specifically, a volume-averaged kinetic model is used in Ref. [9] to study the plasma decay at rather low gas pressures, and, to obtain reasonable agreement with experiment (for T_e values), the energy of superthermal electrons (w^*) had to be reduced by a factor of ~ 20 , from 11 to 0.5 eV (in Ne). Most likely, this can be explained by the energy-transfer rate ($\propto \epsilon_{\text{eff}}^*$) being significantly overestimated.

The second example is that a volume-averaged kinetic model fails to describe correctly the diffusion-cooling rate. Indeed, the model of Ref. [9] predicts that $H_{\text{dc}} \approx -n_e T_e / \tau_{\text{amb}}$, which is significantly lower compared with that obtained using the nonlocal kinetic description, namely, $H_{\text{dc}} \approx -n_e e \Phi_w / \tau_{\text{amb}}$ [see Eq. (38)]. Since the diffusion-cooling mechanism is very important at low gas pressures (see Sec. II D), this may also explain the discrepancies (too high values of T_e predicted) between the model predictions and experimental data observed in Ref. [9].

III. THE FLUID APPROACH AND ITS COMPARISON WITH THE KINETIC DESCRIPTION

The fluid approach is widely used to model discharge plasmas in general, and the afterglow plasma in particular (e.g., Refs. [4–6,2]). The details of the fluid approximation can be found in a number of textbooks on plasma physics (e.g., Refs. [20,28]); here we give only a brief description.

In the fluid approach, the whole electron ensemble (i.e., from $w = 0$ to $w = \infty$) is replaced by an “average” electron, to which unique and unidirectional (i.e., not energy-resolved) particle and energy fluxes are assigned, and the continuity equations are used. Moreover, it is assumed that the EDF is Maxwellian. The electron spatial flux is resolved into the diffusion and drift components:

$$\hat{\Gamma}_e = -\hat{D}_e \nabla n_e + n_e \hat{\mu}_e E, \quad (44)$$

where $\hat{D}_e = \hat{T}_e / (m \langle v_a \rangle)$ and $\hat{D}_e / \hat{\mu}_e = \hat{T}_e / e$, and $\langle \dots \rangle$ denotes averaging over a Maxwellian EDF with \hat{T}_e (henceforward, we will use the ‘‘hat’’ over a quantity X , i.e., \hat{X} , to denote that this quantity is obtained in the fluid approach).

The energy-balance equation takes the well-known form (e.g., Refs. [5,20,28])

$$\frac{\partial}{\partial t} \left[\frac{3}{2} n_e(r) \hat{T}_e(r) \right] = -\nabla \cdot \hat{q}_e + e \hat{\Gamma}_e E + \hat{H}_{ea} + \hat{H}_{inel}, \quad (45)$$

where \hat{H}_{inel} represents the cooling rate in inelastic collisions, such as direct (or stepwise) excitation and ionization, \hat{H}_{ea} is the rate of energy exchange between electrons and atoms

$$\hat{H}_{ea}(r) = -n_e(1 - T_a / \hat{T}_e) \langle w \delta v_a \rangle, \quad (46)$$

where a Maxwellian EDF with \hat{T}_e is assumed and Eq. (40) is employed, \hat{q}_e is the electron heat flux which is expressed in terms of the conduction and convection fluxes

$$\hat{q}_e(r) = -\hat{K}_e \nabla \hat{T}_e + \frac{5}{2} \hat{\Gamma}_e \hat{T}_e, \quad (47)$$

where $\hat{K}_e = \hat{K}_e(n_e, \hat{T}_e) = 5n_e \hat{T}_e / (2m \langle v_a \rangle)$ is the thermal conductivity. The boundary condition at the wall for Eq. (45) becomes

$$\hat{q}_{ew} = (2\hat{T}_e + \Delta \hat{\Phi}_w) \hat{\Gamma}_{ew}, \quad (48)$$

where $\hat{\Gamma}_{ew}$ is the electron flux at the wall ($=n_e v_B$, according to the Bohm boundary condition, see Sec. II C). The first term ($2\hat{T}_e$) in Eq. (48) is the mean kinetic energy lost by Maxwellian electrons to the wall. The second term ($\Delta \hat{\Phi}_w$) in Eq. (48) is the mean kinetic energy lost due to the potential difference between the plasma and the wall; the outward heat flux related to this term represents the diffusion-cooling mechanism resulting from diffusion against the space-charge field in the boundary sheath [see the first term in Eq. (39)].

In order to calculate the potential jump in the boundary sheath $\Delta \hat{\Phi}_w$, an *ad hoc* assumption of a Maxwellian EDF is usually employed, which leads to the familiar expression

$$\Delta \hat{\Phi}_w = (\hat{T}_e / 2e) \ln [M \hat{T}_e / (m T_a)]. \quad (49)$$

The wall potential is now $\hat{\Phi}_w = \hat{\Phi}_{sh} + \Delta \hat{\Phi}_w$, where $\hat{\Phi}_{sh} = (\hat{T}_e / e) \ln \chi$ (see Sec. II C).

The fluid and kinetic approaches differ in a number of respects. Under nonlocal conditions, these differences are not only qualitative, but also quantitative. Here we give some examples.

(i) In the fluid approach, the electron flux $\hat{\Gamma}_e$ is represented in terms of n_e and T_e (and their gradients) [see Eq. (44)] which are parameters for the trapped electrons ($n_f \ll n_e$). However, under nonlocal conditions, the trapped-electron flux is negligible compared with the total electron flux, and practically all the electron flux is due to free diffusion of the unconfined (free) electrons. Moreover, the spatial fluxes of different portions of the EDF may be in different (opposite) directions (see Sec. IV), whereas the fluid ap-

proach predicts that *all* electrons diffuse in the same direction (towards the wall). Hence, the representation of Eq. (44) cannot be justified from a physical point of view.

(ii) By the same reasoning as for point (i), the representation of the electron heat flux \hat{q}_e in terms of the electron temperature and its gradients [see Eq. (47)] is not justified. As an example, due to the high thermal conductivity (i.e., large \hat{K}_e), the electron temperature is spatially uniform [i.e., $\hat{T}_e(r) = \text{const}$], as predicted by the fluid approach; whereas a strong spatial inhomogeneity of T_e can exist, as predicted by the kinetic approach (see Sec. IV).

(iii) Since the assumption of a Maxwellian EDF is made, the fluid approach fails to predict correct values for the wall potential jump $\Delta \hat{\Phi}_w$, and thus for $\hat{\Phi}_w$. Indeed, the kinetic calculations show that the EDF can be strongly non-Maxwellian and that the expression for $\hat{\Phi}_w$ involves the dependence on such important plasma parameters as electron density, pressure, superthermal flux, etc. [see Eq. (34)]. Not only is $\Delta \hat{\Phi}_w$ of Eq. (49) independent of these parameters, but also its value is, as a rule, excessively high (i.e., $\Delta \hat{\Phi}_w \gg T_e / e$). One of the direct impacts of this fact is that the fluid approach significantly overestimates the diffusion-cooling rate ($\propto \hat{\Phi}_w$). Since the diffusion-cooling mechanism is dominant under low pressures, the latter can lead to erroneous predictions of the energy-decay rate, as will be shown in Sec. IV.

(iv) Since the fluid energy-balance equation (45) applies to all electrons (e.g., no distinction is made between trapped and free electrons), it involves the term H_{inel} describing losses of energy in inelastic processes with, in principle, any threshold ϵ^* . In the kinetic energy-balance equation (35), only inelastic processes with thresholds $\epsilon^* \leq e \Phi_w$ are to be included. Since typically (at least for rare gases), the condition that $e \Phi_w < \epsilon^*$ is satisfied, inelastic processes do not affect the energy balance of the trapped electrons. By contrast, the contribution of inelastic processes into the fluid energy balance can be very important (especially in the early afterglow when T_e is high).

(v) By the same reasoning as for point (iv), in the fluid approach, it is not possible to describe correctly the influence of superthermal electrons (e.g., on the wall potential and the diffusion-cooling rate), as well as the heating rate by superthermal electrons, since the electron ensemble is not resolved into different groups (see Sec. II E).

IV. NUMERICAL RESULTS AND DISCUSSION

In order to validate the present method, the full time- and space-dependent kinetic equation (1) was solved numerically in a 1D cylindrical geometry, subject to the boundary conditions (6) and (7). The numerical scheme consisted in writing the kinetic equation in a discrete form and applying a central-difference operator on a 2D (total-energy–radius) grid. The numbers of energy and radial cells were 200–400 and 30–50. The treatment of the e - e collision integral was made by using the discretization method proposed by Rockwood [29] (see also Ref. [30]). [Note that the matrix coefficients corresponding to the e - e collisional integral were obtained by Rockwood for the vf_0 formulation; it is straightforward (though lengthy) to calculate these coeffi-

icients for the f_0 formulation used in the present work (see also Ref. [31].) A similar technique has been used in Ref. [32] for a steady-state positive-column plasma. It should be mentioned that calculations of a steady-state EDF of the trapped electrons have been carried out in Ref. [12] for a 1D geometry and in Ref. [14] for a 2D geometry by employing a space-averaged (nonlocal) kinetic equation which also includes the e - e collisional integral. Basically, due to the strong influence of the e - e collision integral, very small time steps Δt have to be employed to avoid numerical instabilities, i.e., $\Delta t \ll \nu_e^{-1}$. As in Ref. [30], an implicitlike scheme (for the e - e collisional integral) was used which is (in principle) unconditionally stable and allows reasonable time steps. Such a scheme enabled $\Delta t \sim \nu_e^{-1}(\epsilon_{\min})$ to be used, where ϵ_{\min} is the minimum energy of the ϵ grid (typically, $\epsilon_{\min} = T_e/25$ and $\Delta t \sim 10^{-9} - 10^{-8}$ s). The time step Δt was controlled by verifying at every step that the energy-balance equation is satisfied within a relative precision of 10^{-3} , or better. Test runs were performed with different time steps to ensure that the chosen precision is sufficient. In order to allow for the increase in ν_e with time ($\nu_e \propto T_e^{-3/2}$), Δt was decreased dynamically to follow this dependence. However, no special efforts were made to optimize the code and a full kinetic simulation from Eq. (1) of $\sim 50 \mu\text{s}$ into the afterglow took about 3 days of CPU time on a medium-performance workstation. The long computational time can also be explained by the fact that a great number of time steps had to be performed.

We present here simulations for an afterglow in Ar at $p = 0.5$ Torr and at room temperature ($T_a = 300$ K), for $R = 1$ cm. We took $\nu_a = 1.7 \times 10^{10} p(w/\epsilon^*)^{3/2} \text{ s}^{-1}$ from Ref. [17] and $D_i = 40/p \text{ cm}^2 \text{ s}^{-1}$. Under the studied conditions, the inequalities $\lambda_a < \Lambda$ and $\lambda_\epsilon > \Lambda$ are well satisfied at energies of interest (e.g., at $w = 5$ eV, $\lambda_a = 0.06$ cm and $\lambda_\epsilon/\sqrt{\delta} = 10$ cm). Attention is focused primarily on the early afterglow, when T_e is relatively high and the influence of superthermal electrons is not as important as in the late afterglow (e.g., Refs. [27,24,25,22]). Hence, the numerical simulations were performed assuming that there are no metastables present, i.e., $Q^* = 0$. As discussed previously, in the simulations of the EDF decay, we used Eq. (32) to calculate $\Phi(r)$ and Eq. (33) [in which the analytic EDF of Eq. (23) was employed] to find Φ_w . At every time step $t + \Delta t$, $\Phi(r)$ and Φ_w were calculated explicitly, i.e., using the plasma parameters from the previous time step t . Since these formulas involve only the energy-averaged parameters (such as n_e and T_e), which evolve slowly with time, such a procedure is likely to be correct. The fact that $\Phi(r)$ (and hence the integration domain) changes from one time step to another results in a problem of a “moving grid.” However, since very small time steps were used ($\Delta t \sim 10^{-9} - 10^{-8}$ s), $\Phi(r)$ hardly changed in one time step and performing simple (linear) interpolation or extrapolation to update the EDF for each new $\Phi(r)$ proved to be adequate.

In order to initiate a simulation of an afterglow plasma, one has to know the EDF at the start of the afterglow, $t = 0$. In general, it is necessary to start with an EDF which corresponds to the “power-on” period of the discharge (e.g., Ref. [9]) and which can be obtained from a steady-state kinetic equation with a source term (e.g., due to an applied

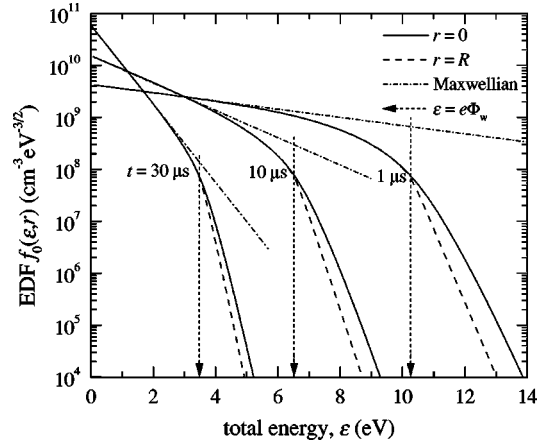


FIG. 1. EDFs at different instants t during the afterglow obtained from the numerical solution of the full kinetic equation (1): the solid lines represent the EDFs at $r=0$ and the dashed lines represent those at $r=R$. The dash-dot lines indicate the Maxwellian parts of the EDF. The vertical arrows show the values of the wall potential energy $\epsilon = e\Phi_w$.

electric field, a microwave power, or an external ionization source). Together with the EDF, all other initial plasma parameters, such as $\Phi(r)$ and Φ_w , at $t=0$ can be found and a smooth transition from the “power-on” period to the “power-off” period can be achieved. Since we do not know such a steady-state EDF, we first chose the initial n_e and T_e and then took the EDF from Eq. (16) (corresponding to these initial n_e and T_e) to be the initial EDF. We also tried other types of EDF (with the same n_e and T_e), such as a single Maxwellian, as well as a bi-Maxwellian for $\epsilon < e\Phi_w$ and $\epsilon > e\Phi_w$. We then observed that the shape of the initial EDF affects only the beginning of the afterglow for $t \lesssim \tau_{fd} \sim 0.1 - 1 \mu\text{s}$. The reason is that once the free electrons of the initial EDF have escaped to the wall (in a short time of $\sim \tau_{fd}$), a flow of electrons out of the potential well ($\epsilon \leq e\Phi_w$) into the free region ($\epsilon > e\Phi_w$) appears and the shape of the initial EDF becomes more or less unimportant. Since our method assumes a quasistationary free EDF, it cannot be applied at the beginning of the afterglow (say when $t \leq 1 \mu\text{s}$) and some discrepancies can be observed during this period. However, since no significant changes in n_e and T_e occur during this period, such discrepancies are not important. By using the initial EDF from Eq. (16), runs with various initial n_e and T_e were carried out, and the case presented here is for typical $n_{e0}(t=0) = 0.3 \times 10^{11} \text{ cm}^{-3}$ and $T_{e0}(t=0) = 3.1$ eV.

Figure 1 depicts the EDFs $f_0(\epsilon, r, t)$ obtained from the full kinetic calculations from Eq. (1) at different instants t during the afterglow. One can see that the trapped EDF ($\epsilon \leq e\Phi_w$) depends essentially on total energy only, and so is spatially homogeneous. On the contrary, the free EDF ($\epsilon > e\Phi_w$) exhibits significant spatial inhomogeneity and is strongly depleted. The whole EDF is thus essentially non-Maxwellian and is close to Maxwellian only at thermal energies (see Fig. 1).

The values of the electron current density at the wall (j_{ew}) obtained from the computed EDFs $f_0(\epsilon, r, t)$ are shown in Fig. 2. The values of the ion current density (j_{iw}) at the wall are also plotted for comparison. One can see that j_{ew} and j_{iw} are in close agreement, which implies that the values of Φ_w

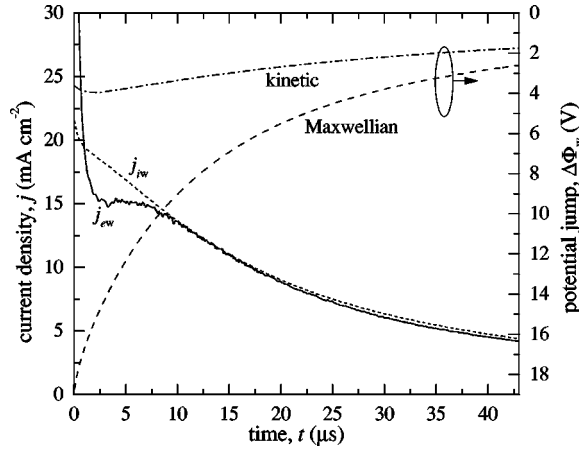


FIG. 2. Total electron (solid line) and ion (short-dashed line) current densities at the wall as functions of time. The dot-dash line represents the values of the potential jump $\Delta\Phi_w$ computed from Eq. (33) using the nonlocal EDF of Eq. (23) (nonlocal kinetic approach). The dashed line shows $\Delta\hat{\Phi}_w$ calculated from Eq. (49) (assumption of a Maxwellian EDF).

are predicted by the present method [see Eq. (33), in which $j_{ew} = j_{iw}$] with good accuracy. Only at the beginning of the afterglow ($t \lesssim 1 \mu\text{s}$), there is a notable discrepancy between j_{ew} and j_{iw} , the reason for which was discussed above. The facts that the dependence of Φ_w on j_{iw} is logarithmic [e.g., see Eq. (34)] and that the difference between j_{ew} and j_{iw} is small ($< 15\%$, see Fig. 2) suggest that the error in predicting Φ_w is even smaller ($\ll 15\%$). Also shown in Fig. 2 are the values of the potential jump $\Delta\Phi_w$ calculated from Eq. (33) (the present kinetic method) and from Eq. (49) (assumption of a Maxwellian EDF) using the same T_e . One can see that the “kinetic” $\Delta\Phi_w$ varies little with time despite the fact that T_e drops dramatically (see below). It is interesting to note that this temporal behavior of $\Delta\Phi_w$ may provide a plausible explanation for the experimental fact that, during an early afterglow, the plasma potential features little variation with time, which was observed in a low-pressure (collisionless) post-discharge plasma [33]. In contrast, the “Maxwellian” $\Delta\hat{\Phi}_w$ decreases markedly with time [it follows the T_e evolution, see Eq. (49)] and is much greater than that obtained in the kinetic approach [Eq. (33)]. By using these (excessive) $\Delta\hat{\Phi}_w$ to calculate the EDF, no reasonable values for j_e could be obtained (these j_e were several orders of magnitude lower than j_i).

The full kinetic simulations of the electron-energy decay were compared with computations from the energy-balance equation (35), in which the nonlocal EDF $f_0^{(0)}(\epsilon)$ was simultaneously calculated from Eq. (23) to obtain the T_e profiles. The advantage of using the energy-balance equation is that the calculations are simple and very fast, which require CPU time of the order of minutes, instead of days, as is the case in full kinetic simulations. In order to simulate the T_e decay from Eq. (35), we took the values of $n_e(r, t)$ and $j_e(r, t)$ predicted by the full kinetic simulations, as well as the values of $T_e(r, t=0)$, $\Phi(r, t)$, and $\Phi_w(t)$ used for these simulations. For the purposes of direct comparison between the fluid and kinetic approaches, computations of $\hat{T}_e(r, t)$ were

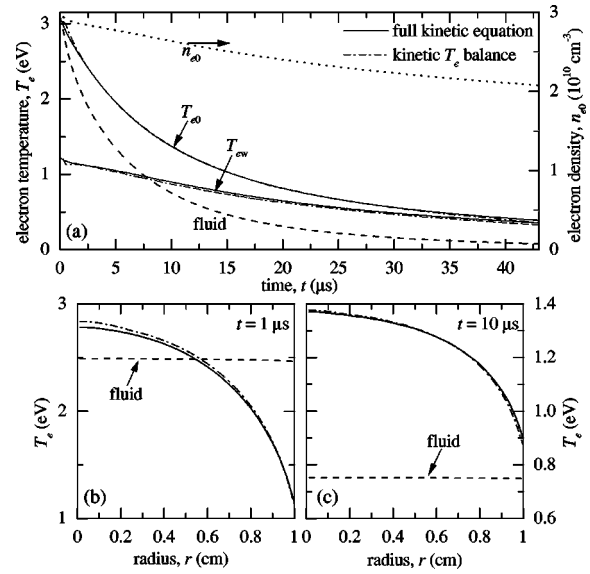


FIG. 3. (a) Time evolution of the electron temperature at the discharge center (T_{e0}) and at the wall (T_{ew}): the solid lines show the full kinetic results from Eq. (1), the dash-dot lines represent the calculations from the kinetic energy-balance equation (35), and the dashed line depicts the calculations from the fluid energy-balance equation (45) (note that the “fluid” T_e profiles feature negligible radial dependence). The dotted-line shows the central electron density (n_{e0}) obtained from Eq. (1). (b) and (c) T_e radial profiles at different instants t : line types are consistent.

also carried out from the fluid energy-balance equation (45), in which $\Delta\hat{\Phi}_w$ was calculated from Eq. (49).

Figure 3(a) depicts the time evolution of the electron temperature at the discharge center (T_{e0}) and at the wall (T_{ew}), as predicted by the full kinetic calculations from Eq. (1). About an order of magnitude decrease in T_e is obtained, whereas the electron density is observed to decrease only by one third. One can see that the time evolution of T_e takes place in two stages. During the first, fast stage ($t < 25 \mu\text{s}$), T_e drops by more than a factor of 5. A significant spatial inhomogeneity of T_e is supported throughout the fast stage; the radial decrease of T_e corresponds to the convex EDF in Fig. 1 and of Eq. (23). The fast stage is followed by a slow stage ($t > 30 \mu\text{s}$), during which the T_e decay rate is substantially lower, the spatial inhomogeneity is less pronounced, and $T_e(r) \approx \bar{T}_e = \text{const}$. For comparison, the values of T_{e0} and T_{ew} predicted by the kinetic energy-balance equation (35) are shown in Fig. 3(a). One can see that they are in good agreement with the full kinetic results, both in their absolute values and spatial profiles [see also Figs. 3(b) and 3(c)]. By contrast, the calculations from the fluid energy-balance equation (45) predict a much faster decay of T_e as compared with the kinetic results, which is mainly due to the fact that the potential jump $\Delta\hat{\Phi}_w$ [see Eq. (49)], and thus the diffusion-cooling rate [$\propto \hat{q}_{ew}$ of Eq. (48)], are significantly overestimated (see Fig. 2 and Sec. III). Moreover, the “fluid” radial profiles of T_e are very flat, as seen in Figs. 3(b) and 3(c), due to the high thermal conductivity. Hence, the fluid approach fails to reproduce not only the spatial behavior of T_e , but also its absolute values.

The radial profiles of the terms in the energy-balance equation of the trapped electrons (as discussed in Sec. II D)

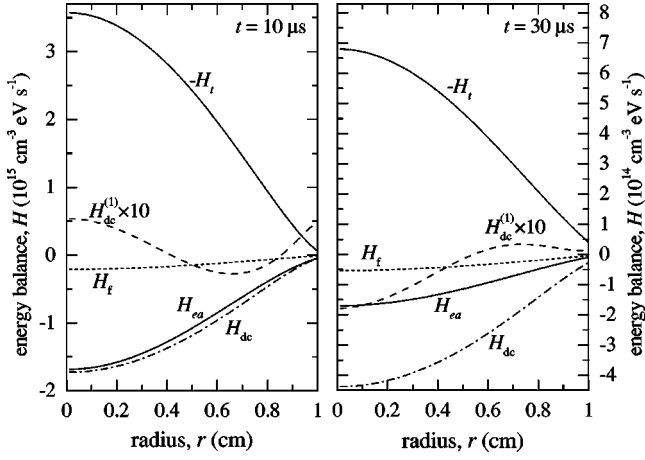


FIG. 4. Radial profiles of the terms in the energy-balance equation (see Sec. IID) obtained from the computed EDFs at two different instants t . Here, $H_t = \partial(\frac{3}{2}n_e T_e)/\partial t$. For clarity, the $H_{dc}^{(1)}$ values are multiplied by a factor of 10.

obtained from the computed EDFs $f_0(\epsilon, r, t)$ are presented in Fig. 4 for two instants t during the afterglow. At early times in the afterglow period, when T_e is high, H_{ea} is comparable with H_{dc} , whereas later, when T_e has dropped, H_{ea} is lower than H_{dc} . Moreover, the cooling rate H_t is small throughout the afterglow period. The rate $H_{dc}^{(1)}$ is also very small and features complicated spatial behavior (determined by $f_0^{(1)}$).

Figure 5 shows the radial profiles of the electron current density j_e at different instants t , as predicted by the full kinetic calculations. Also plotted are the results of calculations

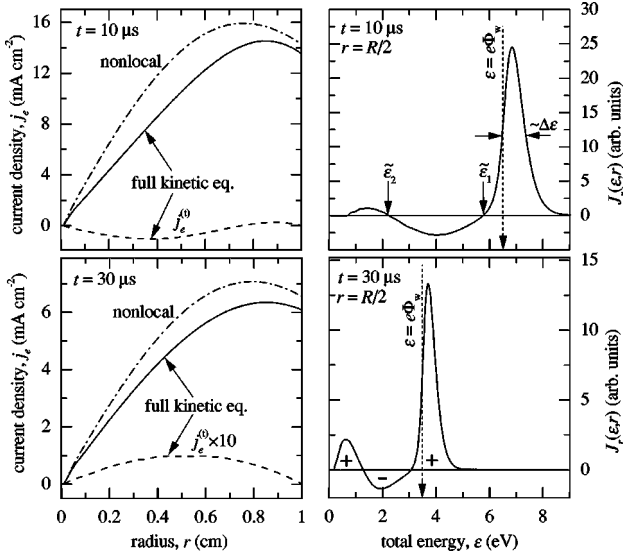


FIG. 5. Radial profiles of the electron current density j_e at different instants t (shown on the left-hand side diagrams): the solid lines represent the full kinetic results from Eq. (1), the dash-dot lines correspond to the calculations from Eq. (28) (nonlocal approach), in which the analytic EDF of Eq. (23) is used, the dashed lines depict the trapped-electron current density $j_e^{(t)}$. The right-hand-side diagrams display the differential spatial flux $J_r(\epsilon, r)$ as a function of total energy at $r=R/2$ and the same instants t . The dashed vertical arrows indicate the values of $\epsilon = e\Phi_w$. The solid vertical arrows show the energies at which the flux reversal takes place.

of $j_e(r)$ from Eq. (28) using the analytic EDF $f_0^{(0)}(\epsilon)$ of Eq. (23). Close agreement (especially at the wall) is observed between $j_e(r)$ from Eq. (28) and that from the full kinetic simulations. It is due to this close agreement between the full kinetic results and those obtained using the nonlocal approach that it becomes possible to calculate Φ_w from Eq. (33) with good accuracy, and thus observe the close correspondence between j_{ew} and j_{iw} in Fig. 2. This represents a striking result of the nonlocal approach which allows the total spatial flux $\Gamma_e(r)$ [or $j_e(r)$] to be calculated in terms of the differential energy flux $J_e(\epsilon, r)$ at $\epsilon = e\Phi_w$ [see Eq. (28)] via the space-independent EDF $f_0^{(0)}(\epsilon)$. Such a relationship between $\Gamma_e(r)$ and $f_0^{(0)}(\epsilon)$ is possible because $f_0^{(0)}(\epsilon)$ contains all required space-resolved information (e.g., Refs. [11,15]). The transformation [described by Eq. (24)] from the energy flux out of the potential well (J_e at $\epsilon = e\Phi_w$) into the spatial flux (Γ_e) occurs in the narrow energy region close to $e\Phi_w$, in which the differential spatial flux $J_r(\epsilon, r)$ is peaked; see the right-hand side diagrams in Fig. 5, where $J_r(\epsilon, r)$ is plotted as a function of total energy at $r=R/2$ (its energy dependence is similar at other radii). Simple arguments suggest that the main contribution to the electron current is due to the free electrons with $e\Phi_w < \epsilon \leq e\Phi_w + \Delta\epsilon$. Hence, the characteristic width of the J_r peak is of the order of $\Delta\epsilon$ [see Eq. (22)], as confirmed by the numerical results.

One can next see in Fig. 5 that J_r for the trapped electrons ($\epsilon \leq e\Phi_w$) is nonnegligible in magnitude and, which is very interesting, changes sign. It is clear that the total spatial electron flux Γ_e (integral of J_r over w from 0 to ∞) must be directed outward (to the wall) as is the ion flux Γ_i , i.e., $\Gamma_e > 0$. For the free electrons with $\epsilon > e\Phi_w$ (whose contribution to Γ_e is the largest), indeed, $J_r(\epsilon, r) > 0$. For the trapped electrons, however, J_r is inwardly directed ($J_r < 0$) for some energies and is outwardly directed ($J_r > 0$) for other energies. It is due to the (partial) compensation of these oppositely directed fluxes for $\epsilon \leq e\Phi_w$ that $j_e^{(t)} (= e\Gamma_e^{(t)})$ is small (see Fig. 5). The sign of $j_e^{(t)}$ depends on whether the inwardly directed flux for $\epsilon \leq e\Phi_w$ is greater or smaller than the outwardly directed flux. We observed that $j_e^{(t)}$ was oppositely directed to j_e for $t \lesssim 20 \mu s$, while later ($t \gtrsim 20 \mu s$), j_e and $j_e^{(t)}$ had the same sign (see Fig. 5 for data at $t = 10 \mu s$ and $t = 30 \mu s$).

One can observe in Fig. 5 that there are actually two flux (J_r) reversals (changes of sign), one at $\epsilon = \tilde{\epsilon}_1$ close to $e\Phi_w$ and the other at lower (thermal) energies, $\epsilon = \tilde{\epsilon}_2$. In the nonlocal approach, the small perturbation term $f_0^{(1)}(\epsilon, r)$ is responsible for a nonzero spatial flux of trapped electrons (and its sign), and the main term $f_0^{(0)}(\epsilon)$ (which is responsible for their energy fluxes) yields a zero spatial flux. By using Eq. (24), which connects the spatial and energy fluxes, it is possible to explain the observed flux reversals, as discussed briefly in the rest of this section.

The first flux reversal occurs at energies close to $e\Phi_w$, i.e., $\epsilon = \tilde{\epsilon}_1 < e\Phi_w$. By virtue of Eq. (24), the sign of $J_r(\epsilon, r)$ [$\equiv J_r^{(1)}(\epsilon, r)$ for $\epsilon \leq e\Phi_w$] is determined (to some extent) by that of $\mathcal{J}_\epsilon = \partial(\sqrt{w}J_e^{(0)})/\partial\epsilon$. Since the EDF falls rapidly in the vicinity of $\epsilon \approx e\Phi_w$ (see Fig. 1), its local slope decreases, and it is possible to show that $|J_e^{(0)}(\epsilon)|$ has a

maximum at $\epsilon = \tilde{\epsilon}_1 \approx e\Phi_w - T_e$. As such, $\mathcal{J}_\epsilon(\epsilon)$ [and thus $J_r(\epsilon)$] changes sign at $\epsilon = \tilde{\epsilon}_1$; hence $J_r(\epsilon)$ for $\epsilon < \tilde{\epsilon}_1$ becomes inwardly directed ($J_r < 0$). Physically, the position of the first flux reversal, $\tilde{\epsilon}_1$, corresponds to the energy at which the trapped electrons start to feel the spatial gradients due to the presence of the wall; at this energy the transformation from the energy flux J_ϵ to the spatial flux J_r starts to occur and the magnitude of J_ϵ begins to diminish with increasing energy.

The second flux reversal occurs at thermal energies $\epsilon = \tilde{\epsilon}_2 \lesssim (3-4)T_e$. This flux reversal is due to a particular property of the e - e collision integral at thermal energies, namely, due to the fact that the coefficient A_1 (and A_2) of Eq. (4) is an increasing function of energy for $w \lesssim (3-4)T_e$. Indeed, taking into account that $v_e \gg \delta v_a$ at thermal energies, $v_e(w) \propto w^{-3/2}$, and $A_1(w) \propto w$ when $w \lesssim 2.6\tilde{T}_e$ [see Eq. (4)], one can obtain that $\sqrt{w}J_\epsilon^{(0)} \propto w \exp(-\epsilon/\tilde{T}_e)$. As such, it is easy to see that $\mathcal{J}_\epsilon(\epsilon)$ [and thus $J_r(\epsilon)$] changes sign; hence $J_r(\epsilon)$ for $\epsilon < \tilde{\epsilon}_2$ becomes outwardly directed again ($J_r > 0$). As a rough estimate, $\tilde{\epsilon}_2 \approx \tilde{T}_e + \langle e\Phi \rangle$, which was observed to be in reasonable agreement with the numerical results.

To conclude, the above results show that a situation is realized, in which the radial fluxes corresponding to three different portions of the EDF alternate in sign (cf., the fluid approach in which the electron flux is unidirectional, see Sec. III). Large, directionally opposed radial fluxes of trapped electrons exist, and two flux reversals occur. The flux reversal at thermal energies was predicted in terms of the general properties of the e - e collision integral. This phenomenon can hence be considered to be somewhat universal and likely to take place in other plasmas (under nonlocal conditions) where e - e Coulomb collisions are effective in maintaining a Maxwellian EDF at thermal energies. Note that we also observed this phenomenon (which was even more pronounced) in a steady-state negative-glow plasma, on which a separate report is under preparation.

V. SUMMARY AND CONCLUSIONS

The nonlocal electron kinetics is studied in a low-pressure afterglow plasma. A method based on the nonlocal approach is reported, which allows one to simplify greatly the problem and to account properly for the nonlocal nature of the EDF.

The method consists in solving simplified (nonlocal) kinetic equations coupled with particle- and energy-balance equations. The applicability of the proposed method was validated by the numerical solution of the full time- and space-dependent kinetic equation in a cylindrical geometry. Good agreement is found between the full kinetic simulations and the results obtained from the kinetic energy-balance equation. Since the nonlocal approach reduces a multidimensional kinetic equation to a 1D nonlocal kinetic equation in (genuine) total energy, the proposed method can be easily extended to geometries other than cylindrical. Moreover, the proposed method being simple and semianalytic, its computational efficiency can be extremely useful in solving complex self-consistent problems.

It is shown that under nonlocal conditions the EDF can be strongly non-Maxwellian and that the *ad hoc* assumption of a Maxwellian EDF can lead to significant errors. The results of the direct comparison between the fluid and kinetic approaches imply that the fluid approach is physically inappropriate for describing a low-pressure afterglow plasma. In particular, the fluid approach fails to predict correctly both the spatial and temporal evolution of the electron temperature. Moreover, it is demonstrated that the use of the volume-averaged (zero-dimensional) kinetic models may lead to erroneous results in simulating such a plasma.

The present results for a low-pressure (collisional) afterglow plasma can be somewhat extended to the high-density, low-pressure (collisionless) afterglow plasmas, which typically operate at $n_e \sim 10^{11} - 10^{12} \text{ cm}^{-3}$ and $p < 10 - 100$ mTorr (e.g., Refs. [7,1,2]). At such high densities, e - e Coulomb collisions may become more effective in driving the EDF to a Maxwellian distribution. On the other hand, at such low pressures, the removal rate of electrons to the wall is expected to be much higher. Hence, the high-density, low-pressure (collisionless) plasmas are also likely to feature, among other things, a strong departure from a Maxwellian distribution. This subject will be explored in future work.

ACKNOWLEDGMENTS

The authors are grateful to L. D. Tsendin for stimulating discussions and insight, and for carefully reading and commenting on the manuscript. R.R.A. thanks R. C. Tobin for his continuous support and encouragement. The work of A.A.K. was supported in part by INTAS Grant No. 96-0235.

-
- [1] M. A. Lieberman and S. Ashida, *Plasma Sources Sci. Technol.* **5**, 145 (1996).
 - [2] D. P. Lymberopoulos, V. I. Kolobov, and D. J. Economou, *J. Vac. Sci. Technol. A* **16**, 564 (1998).
 - [3] S. A. Gutsev, A. A. Kudryavtsev, and V. A. Romanenko, *Tech. Phys.* **40**, 1131 (1995).
 - [4] J. W. Poukey, J. B. Gerardo, and M. A. Gusinow, *Phys. Rev.* **179**, 211 (1969).
 - [5] A. K. Bhattacharya and J. H. Ingold, *J. Appl. Phys.* **43**, 1535 (1972).
 - [6] D. Trunec, P. Španěl, and D. Smith, *Contrib. Plasma Phys.* **34**, 69 (1994).
 - [7] S. Ashida, C. Lee, and M. A. Lieberman, *J. Vac. Sci. Technol. A* **13**, 2498 (1995).
 - [8] C. Gorse, M. Capitelli, M. Bacal, J. Bretagne, and A. Laganá, *Chem. Phys.* **117**, 177 (1987).
 - [9] T. Bräuer, S. Gortchakov, D. Loffhagen, S. Pfau, and R. Winkler, *J. Phys. D* **30**, 3223 (1997).
 - [10] I. B. Bernstein and T. Holstein, *Phys. Rev.* **94**, 1475 (1954).
 - [11] L. D. Tsendin, *Sov. Phys. JETP* **39**, 805 (1974).

- [12] U. Kortshagen, *J. Phys. D* **26**, 1691 (1993).
- [13] U. Kortshagen, I. Pukropski, and L. D. Tsendin, *Phys. Rev. E* **51**, 6063 (1995).
- [14] V. I. Kolobov and W. N. G. Hitchon, *Phys. Rev. E* **52**, 972(1995).
- [15] U. Kortshagen, C. Busch, and L. D. Tsendin, *Plasma Sources Sci. Technol.* **5**, 1 (1996).
- [16] U. Kortshagen, G. J. Parker, and J. E. Lawler, *Phys. Rev. E* **54**, 6746 (1996).
- [17] V. I. Kolobov, G. J. Parker, and W. N. G. Hitchon, *Phys. Rev. E* **53**, 1110 (1996).
- [18] R. R. Arslanbekov and A. A. Kudryavtsev, in *Electron Kinetics and Applications of Glow Discharges*, Vol. 367 of *NATO Advanced Study Institute Series B: Physics*, edited by U. Kortshagen and L. D. Tsendin (Plenum, New York, 1998), pp. 161–178.
- [19] L. D. Tsendin, in *Electron Kinetics and Applications of Glow Discharges*, Vol. 367 of *NATO ASI Series B: Physics*, edited by U. Kortshagen and L. D. Tsendin (Plenum, New York, 1998), pp. 1–18.
- [20] V. E. Golant, A. P. Zhilinsky, and I. E. Sakharov, *Fundamentals of Plasma Physics* (Wiley, New York, 1980).
- [21] A. I. Korotkov, A. A. Kudryavtsev, and N. A. Khromov, *Tech. Phys.* **41**, 1020 (1996).
- [22] N. B. Kolokolov, A. A. Kudryavtsev, and A. B. Blagoev, *Phys. Scr.* **50**, 371 (1994).
- [23] L. L. Alves, G. Gousset, and C. M. Ferreira, *Phys. Rev. E* **55**, 890 (1997).
- [24] A. B. Blagoev, Y. M. Kagan, N. B. Kolokolov, and R. I. Lyagushchenko, *Sov. Phys. Tech. Phys.* **19**, 215 (1974).
- [25] N. B. Kolokolov, A. A. Kudryavtsev, and O. G. Toronov, *Sov. Phys. Tech. Phys.* **30**, 1128 (1985).
- [26] A. P. Zhilinskii, I. F. Liventseva, and L. D. Tsendin, *Sov. Phys. Tech. Phys.* **22**, 177 (1977).
- [27] J. C. Ingraham and S. C. Brown, *Phys. Rev.* **138**, 1015 (1965).
- [28] M. A. Lieberman and A. J. Lichtenberg, *Principles of Plasma Discharges and Materials Processing* (Wiley, New York, 1994).
- [29] S. D. Rockwood, *Phys. Rev. A* **8**, 2348 (1973).
- [30] C. J. Elliott and A. E. Greene, *J. Appl. Phys.* **47**, 2946 (1976).
- [31] J. Bretagne, J. Godart, and V. Puech, *J. Phys. D* **15**, 2205 (1982).
- [32] M. J. Hartig and M. J. Kushner, *J. Appl. Phys.* **73**, 1080 (1993).
- [33] M. B. Hopkins and W. G. Graham, *J. Appl. Phys.* **69**, 3461 (1991).